Research in Dynamical Astronomy and the Quest for Planet Nine

William Moll
Seton Hall University

Donna D'Alessio
Seton Hall University

Research in Dynamical Astronomy and the Quest for Planet Nine

William Moll and Donna D'Alessio
Seton Hall University

Abstract

The field of dynamical systems theory, greatly advanced by Henri Poincaré in the late 19th century, has made invaluable contributions to celestial mechanics, helping to describe motion in the solar system and beyond. Poincaré famously employed the techniques of dynamical systems to address the Three-Body Problem. In recent years, a myriad of research has addressed the possibility of the existence of a new planet ("Planet Nine") beyond Neptune, based on evidence from the unique structure of various objects observed in the Kuiper Belt. Initial research out of the California Institute of Technology has engendered significant controversy over concerns of selection bias and lack of evidence, despite claims of a high level of certainty in their results. We created simulations in Wolfram's Mathematica and Universe Sandbox to visualize and further study perturbations caused by Planet Nine on numerous objects in the Kuiper Belt. A Lagrange contour plot was produced in Python to observe Planet Nine's possible effect on the solar system. From this research, the existence of Planet Nine cannot be positively established, but a better understanding of the dynamics of a system including Planet Nine can be achieved through the use of simulations and dynamical studies.

1. Introduction

In undertaking this project, we embarked with the goals of achieving a better understanding of dynamical systems theory, delving into the world of mathematical astronomy, and exploring an ongoing scientific controversy. With our sights locked on outer space, Planet Nine research came into view as a way to advance our knowledge of mathematics and astronomy as well as perhaps make a modest contribution to an open scientific question. Within the last decade, hypotheses about a distant planet beyond Neptune have taken shape and evolved into a more realistic proposition than initially believed. Upon the inspection of clustered argument of perihelion (ω) measurements in a number of Kuiper Belt objects, hypotheses from the early 2000s resurfaced in the form of a Trans-Neptunian perturber in the solar system (Trujillo & Sheppard, 2014). Following these observations, Batygin & Brown (2016) examined the evidence for this distant planet, supporting the idea *mathematically*. Given the estimated distance of this planet from the Sun, more than two orders of magnitude larger than that of Earth, a mathematical approach is the best that can be applied at this time. Fortunately, mathematics and astronomy have a storied history that is centuries old.

The remainder of this paper is structured as follows: Section 1.1 provides an overview of the necessary dynamical systems background, and

Section 1.2 then reviews the history of Planet Nine investigations. Section 2 presents our methods and Sections 3 and 4 then present, respectively, a discussion and our conclusions.

1.1. Mathematical Foundations

Dynamical systems provide a functional description of the solution of a mathematical model describing a problem, e.g., the motion of bodies in outer space. Dynamical systems theory is a mathematical formalization that defines a state space, a set of times, and an evolution rule. The state space may be finite or infinite, as well as continuous or discrete. For a continuous system, the set of observations can be either discrete (and typically regular in time or some other parameter such as angle) or itself continuous. The evolution rule may be deterministic or stochastic, as well as autonomous or time-dependent. Differential equations are typically used to define a continuous-time dynamical system. Perko (2001) defines a dynamical system as a function $\phi(t, x)$, defined for all $t \in \mathbb{R}, x \in E \subset \mathbb{R}^n$. This describes how the points $x \in E$ evolve with time. A dynamical system on E is a C^1-map

$$\phi : \mathbb{R} \times E \to E \qquad (1)$$

where E is an open subset of $\mathbb{R}^n$ and if $\phi_t(x) = \phi(t, x)$, then ϕ_t satisfies the following:

$$\phi_0(x) = x \qquad \forall \quad x \in E$$
$$\phi_t \circ \phi_s = \phi_{t+s} \qquad \forall \quad s, t \in \mathbb{R}, x \in E.$$

Note that if the system evolves from an initial configuration, $\mathbb{R}$ can be replaced by $\mathbb{R}^{\geq 0}$. Celestial motion is a classical example of such a system. In fact, problems in dynamical astronomy have motivated many of the developments in dynamical systems theory.

Modern celestial mechanics owes much to the pioneering work of Johannes Kepler. His research led to the modern laws of planetary orbits and modified the heliocentric theory of Canon Nicolaus Copernicus. Kepler realized that planetary orbits were elliptical rather than circular with epicycle, as had been previously believed, and also explained how planetary velocities vary. The Kepler Problem is a special case of the Two-Body Problem, in which the two bodies interact by a gravitational force that varies in strength as the inverse square of the distance between them (Kepler & Donahue, 2015). Sir Isaac Newton et al. (1999) continued to advance the field with his three laws of motion and his law of universal gravitation, his contributions providing a more rigorous foundation for Kepler's laws.

Following Newton, Joseph-Louis Lagrange (1811) rigorously studied the Three-Body Problem, i.e., considering the initial positions and velocities (or momenta) of three point masses and solving for their subsequent motion according to Newton's laws. However, unlike the Two-Body Problem, no general closed-form solution exists when a third object is introduced. Lagrange also analyzed the stability of planetary orbits, and discovered the existence of Lagrangian points, also known as L-points, or libration points. L-points are points of equilibrium for small-mass objects under the influence of two massive orbiting bodies. Lagrangian mechanics is a reformulation of classical mechanics. Rather than focusing on "force," Lagrange's approach emphasizes "energy" and is based on the principle of stationary action. He developed a method by which a single polar coordinate equation could be used to describe any orbit.

In this restricted Three-Body Problem, it is well known that there are five Lagrange points to mirror the two-body case as the third mass is neglected. These points are studied for their stability to see if perturbations will affect the path of an object that would otherwise remain at the equilibrium point. The stability of Lagrange points four and five in particular is a topic of debate. The finding of asteroids or other celestial bodies at L_4 and L_5 in almost all planet-star systems seems to imply that these two Lagrange points are stable. With further examination, however, it is determined that

this is not always the case. For these points to be stable, the heaviest mass, m_1, must be substantially heavier than the second heaviest mass, m_2. To find the Lagrange points, one must consider the bodies in a rotating frame of reference, where two heavier masses m_1 and m_2 do not move. The distance between m_1 and m_2 will be R, therefore, the two heavier masses' positions are:

$$\mathbf{r}_1 = \left(-\frac{m_2 R}{m_1 + m_2}, 0, 0\right),$$
$$\mathbf{r}_2 = \left(\frac{m_1 R}{m_1 + m_2}, 0, 0\right) \tag{2}$$

The angular frequency of the rotating frame of reference, Ω, will only hold because we consider a circular restricted 3-body problem defined as:

$$\Omega^2 R^3 = G(m_1 + m_2) \tag{3}$$

The Lagrange points, L_4 and L_5, are obtained by:

$$L_4 = \left(\frac{R}{2}\left(\frac{m_1 - m_2}{m_1 + m_2}\right), \frac{\sqrt{3}}{2}R, 0\right),$$
$$L_5 = \left(\frac{R}{2}\left(\frac{m_1 - m_2}{m_1 + m_2}\right), -\frac{\sqrt{3}}{2}R, 0\right) \tag{4}$$

It is important to look at the generalized potential about the mass m_3 to find the dynamical stability of motion near the equilibrium points. To find this, we will add the coriolis acceleration and the centrifugal acceleration because we are observing in a rotating frame. Let $\mathbf{r}$ be the position vector of m_3 and Ω the angular velocity such that $\Omega = (0, 0, \Omega)$. Let d_1 and d_2 be the distances between m_3 and m_1 and m_3 and m_2, respectively.

$$d_1^2 = \left(x + \frac{m_2 R}{m_1 + m_2}\right)^2 + y^2 + z^2,$$
$$d_2^2 = \left(x - \frac{m_1 R}{m_1 + m_2}\right)^2 + y^2 + z^2 \tag{5}$$

Therefore, the total acceleration, $\ddot{\mathbf{r}}$, and the generalized potential, U, are calculated by:

$$\ddot{\mathbf{r}} = -\frac{Gm_1(\mathbf{r} - \mathbf{r_1})}{d_1^3} - \frac{Gm_2(\mathbf{r} - \mathbf{r_2})}{d_2^3}$$
$$- 2\Omega \times \dot{\mathbf{r}} - \Omega \times \Omega \times \mathbf{r}$$
$$U = -\frac{Gm_1}{d_1} - \frac{Gm_2}{d_2} \tag{6}$$
$$- 2\Omega(x\dot{y} - y\dot{x}) - \frac{\Omega^2}{2}\left(x^2 + y^2\right)$$

The potential, in addition to position, is dependent on velocity. It must be taken into consideration for the stability of the Lagrange points, even though it does not affect their positions. Therefore, we must separate the components that are dependent on velocity to obtain:

$$U' = U + 2\Omega(x\dot{y} - y\dot{x})$$
$$= -\frac{Gm_1}{d_1} - \frac{Gm_2}{d_2} - \frac{\Omega^2}{2}\left(x^2 + y^2\right) \tag{7}$$

We get the following when we reduce Equation (7) by components:

$$\ddot{x} = -\frac{Gm_1\left(x + \frac{m_2 R}{m_1 + m_2}\right)}{d_1^3} - \frac{Gm_2\left(x - \frac{m_1 R}{m_1 + m_2}\right)}{d_2^3}$$
$$+ 2\Omega\dot{y} + \Omega^2 x$$
$$= -\frac{\partial U'}{\partial x} + 2\Omega\dot{y}$$
$$\ddot{y} = -\frac{Gm_1 y}{d_1^3} - \frac{Gm_2 y}{d_2^3} - 2\Omega\dot{x} + \Omega^2 y \tag{8}$$
$$= -\frac{\partial U'}{\partial y} - 2\Omega\dot{x}$$
$$\ddot{z} = -\frac{Gm_1 z}{d_1^3} - \frac{Gm_2 z}{d_2^3}$$
$$= -\frac{\partial U'}{\partial z}$$

Using the Taylor series expansion of U' around the Lagrange point (x_0, y_0, z_0), we rewrite the generalized potential as a sum of partial derivatives and

are left with:

$$
\begin{aligned}
U' = {}& U_0' + U_x'(x - x_0) + U_y'(y - y_0) \\
& + U_z'(z - z_0) + \frac{1}{2}\Big[U_{xx}'(x - x_0)^2 \\
& + U_{yy}'(y - y_0)^2 + U_{zz}'(z - z_0)^2\Big] \\
& + U_{xy}'(x - x_0)(y - y_0) \\
& + U_{xz}'(x - x_0)(z - z_0) \\
& + U_{yz}'(y - y_0)(z - z_0)
\end{aligned} \tag{9}
$$

where $U_0' = U'|_{(x_0,y_0,z_0)}$ and $U_X' = \frac{\partial U}{\partial X}\Big|_{(x_0,y_0,z_0)}$ for any variable X. However, note that $U_{xz} = U_{yz} = 0$ and that for Lagragange points $U_x' = U_y' = U_z' = 0$. Thus,

$$
\begin{aligned}
U' = {}& U_0' + \frac{1}{2}\Big[U_{xx}'(x - x_0)^2 \\
& + U_{yy}'(y - y_0)^2 + U_{zz}'(z - z_0)^2\Big] \\
& + U_{xy}'(x - x_0)(y - y_0)
\end{aligned} \tag{10}
$$

We linearize the equations of motion and look at the small perturbations to analyze the stability about the equilibrium points in a system. The Lagrange points are fixed points because of the reference frame. The following equations are given:

$$
\begin{array}{cc}
x = x_0 + \delta x & \dot{x} = \delta \dot{x} \\
y = y_0 + \delta y & \dot{y} = \delta \dot{y} \\
z = z_0 + \delta z & \dot{z} = \delta \dot{z}
\end{array} \tag{11}
$$

When we plug these values into (10), we acquire:

$$
\begin{aligned}
U' = {}& U_0' + \frac{1}{2}\Big[U_{xx}'(\delta x)^2 + U_{yy}'(\delta y)^2 \\
& + U_{zz}'(\delta z)^2\Big] + U_{xy}'\delta x\delta y
\end{aligned} \tag{12}
$$

Using (8) and (12), we get:

$$
\begin{aligned}
\delta\ddot{x} &= -U_{xx}'\delta x - U_{xy}'\delta y + 2\Omega\delta\dot{y} \\
\delta\ddot{y} &= -U_{yy}'\delta y - U_{xy}'\delta x - 2\Omega\delta\dot{x} \\
\delta\ddot{z} &= -U_{zz}'\delta z
\end{aligned} \tag{13}
$$

Therefore, we obtain the following:

$$
\frac{d}{dt}\begin{pmatrix} x \\ y \\ z \\ \dot{x} \\ \dot{y} \\ \dot{z} \end{pmatrix} = \frac{d}{dt}\begin{pmatrix} \delta x \\ \delta y \\ \delta z \\ \delta \dot{x} \\ \delta \dot{y} \\ \delta \dot{z} \end{pmatrix} = M \begin{pmatrix} \delta x \\ \delta y \\ \delta z \\ \delta \dot{x} \\ \delta \dot{y} \\ \delta \dot{z} \end{pmatrix} \tag{14}
$$

where the matrix M is given by

$$
M = \begin{pmatrix}
0 & 0 & 0 & 1 & 0 & 0 \\
0 & 0 & 0 & 0 & 1 & 0 \\
0 & 0 & 0 & 0 & 0 & 1 \\
-U_{xx}' & -U_{xy}' & 0 & 0 & 2\Omega & 0 \\
-U_{xy}' & -U_{yy}' & 0 & -2\Omega & 0 & 0 \\
0 & 0 & -U_{zz}' & 0 & 0 & 0
\end{pmatrix}.
$$

We will start by considering only the z-direction. All Lagrange points are stable in the z-direction. To prove this, we will let $\delta x = \delta y = 0$. Using (13), it is determined that δz and $\delta\dot{z}$ are independent of $\delta x, \delta\dot{x}, \delta y$, and $\delta\dot{y}$ and vice-versa, so we can reduce the matrix to:

$$
\frac{d}{dt}\begin{pmatrix} \delta z \\ \delta \dot{z} \end{pmatrix} = \begin{pmatrix} 0 & 1 \\ -U_{zz}' & 0 \end{pmatrix}\begin{pmatrix} \delta z \\ \delta \dot{z} \end{pmatrix}
$$

We have that:

$$
U_{zz}' = \frac{Gm_1}{d_1^3} + \frac{Gm_2}{d_2^3} \tag{15}
$$

by the $\ddot{z}$ equation from (8). Now we have $d_1, d_2 > 0$ and thus $U_{zz}' > 0$ because d_1, d_2 are distances. The eigenvalues of the matrix above are:

$$
\pm i\sqrt{U_{zz}'}.
$$

It is important to note the following corollaries:

Theorem 1.1. *Given a system $X'(t) = AX(t)$ where A has distinct paired complex eigenvalues, $\alpha_1 + i\beta_1, \alpha_1 - i\beta_1 \ldots, \alpha_k + i\beta_k, \alpha_k - i\beta_k$. Let T be the matrix such that $T^{-1}AT$ is in canonical form:*

$$
T^{-1}AT = \begin{pmatrix} B_1 & & \\ & \ddots & \\ & & B_k \end{pmatrix}
$$

where

$$B_i = \begin{pmatrix} \alpha_i & \beta_i \\ -\beta_i & \alpha_i \end{pmatrix}$$

Then, the general solution of $X'(t) = AX(t)$ is $TY(t)$ where

$$Y(t) = \begin{pmatrix} a_1 e^{\alpha_1 t} \cos\beta_1 t + b_1 e^{\alpha_1 t} \sin\beta_1 t \\ -a_1 e^{\alpha_1 t} \sin\beta_1 t + b_1 e^{\alpha_1 t} \cos\beta_1 t \\ \vdots \\ a_k e^{\alpha_k t} \cos\beta_k t + b_k e^{\alpha_k t} \sin\beta_k t \\ -a_k e^{\alpha_k t} \sin\beta_k t + b_k e^{\alpha_k t} \cos\beta_k t \end{pmatrix}$$

Corollary 1.1.1. *A point in a dynamical system whose matrix of equations of motion, A, has an eigenvalue with positive real part is unstable.*

Corollary 1.1.2. *A point in a dynamical system whose matrix of equations of motion, A, has purely imaginary (non-zero) eigenvalues is stable.*

Because the eigenvalues are imaginary, by Corollary 1.1.2, it is understood that the point is stable, and it can be concluded that all Lagrange points are stable in the z-direction.

We can then consider only the x and y directions in the same way we were able to consider only the z-direction. The equation then becomes:

$$\frac{d}{dt}\begin{pmatrix} \delta x \\ \delta y \\ \delta \dot{x} \\ \delta \dot{y} \end{pmatrix} = M_{xy}\begin{pmatrix} \delta x \\ \delta y \\ \delta \dot{x} \\ \delta \dot{y} \end{pmatrix} \quad (16)$$

where the matrix M_{xy} is given by

$$M_{xy} = \begin{pmatrix} 0 & 0 & 1 & 0 \\ 0 & 0 & 0 & 1 \\ -U'_{xx} & -U'_{xy} & 0 & 2\Omega \\ -U'_{xy} & -U'_{yy} & -2\Omega & 0 \end{pmatrix}.$$

The corresponding theorem and its proof are as follows (Greenspan, 2014):

Theorem 1.2. *The Lagrange points L_4 and L_5 are stable in all directions if and only if:*

$$\frac{m_1}{m_2} \geq \frac{25 + 3\sqrt{69}}{2} \approx 24.9599 \quad (17)$$

Proof. To prove this, we start by using (7) to compute the partial derivatives found in (16). Recall that for L_4 and L_5, we have $d_1 = d_2 = R$. Therefore when we evaluate the partial double derivatives at L_4 and L_5, we obtain:

$$U'_{xx} = \frac{Gm_1}{d_1^3} + \frac{Gm_2}{d_2^3}$$
$$- \frac{3Gm_1\left(x + \frac{m_2 R}{m_1 + m_2}\right)^2}{d_1^5}$$
$$- \frac{3Gm_2\left(x - \frac{m_1 R}{m_1 + m_2}\right)^2}{d_2^5} - \Omega^2$$

which, evaluated at $x = \frac{R}{2}\left(\frac{m_1 - m_2}{m_1 + m_2}\right)$, gives

$$= \frac{Gm_1}{R^3} + \frac{Gm_2}{R^3}$$
$$- \frac{3Gm_1\left(\frac{(m_1 + m_2)R}{2(m_1 + m_2)}\right)^2}{R^2}$$
$$- \frac{3Gm_2\left(\frac{-(m_1 + m_2)R}{2(m_1 + m_2)}\right)^2}{R^2} - \Omega^2$$
$$= \frac{1}{4}\frac{G(m_1 + m_2)}{R^3} - \Omega^2$$

$$ \quad (18)$$

$$U'_{yy} = \left(\frac{Gm_1}{d_1^3} + \frac{Gm_2}{d_2^3} - \frac{3Gm_1 y^2}{d_1^5}\right.$$
$$\left. - \frac{3Gm_2 y^2}{d_2^5} - \Omega^2\right)$$

which, evaluated at $y = \pm\frac{\sqrt{3}}{2}R$, gives

$$= \frac{G(m_1 + m_2)}{R^3} - \frac{3Gm_1\left(\frac{3}{4}R^2\right)}{R^5}$$
$$- \frac{3Gm_2\left(\frac{3}{4}R^2\right)}{R^5} - \Omega^2$$
$$= -\frac{5}{4}\frac{G(m_1 + m_2)}{R^3} - \Omega^2$$

$$ \quad (19)$$

and finally,

$$U'_{xy} = -\frac{3Gm_1\left(x+\frac{m_2R}{m_1+m_2}\right)y}{d_1^5}$$
$$-\frac{3Gm_2\left(x-\frac{m_1R}{m_1+m_2}\right)y}{d_2^5}$$

which, evaluated at the same x and y values as before, yields

$$= \mp\frac{3Gm_1\left(\frac{R}{2}\right)\frac{\sqrt{3}}{2}R + 3Gm_2\left(-\frac{R}{2}\right)\frac{\sqrt{3}}{2}R}{R^5}$$
$$= \mp\frac{3\sqrt{3}G(m_1-m_2)}{4R^3}$$
$$= -\frac{3\sqrt{3}}{4}\kappa_\pm\frac{G(m_1+m_2)}{R^3}$$

$$(20)$$

where $\kappa_\pm = \pm(m_1-m_2)/(m_1+m_2)$. Using the definition from Equation (3) of a circular restricted Three-Body Problem, we get:

$$U'_{xx} = -\frac{3}{4}\Omega^2,$$
$$U'_{yy} = -\frac{9}{4}\Omega^2, \qquad (21)$$
$$U'_{xy} = -\frac{3\sqrt{3}}{4}\kappa_\pm\Omega^2.$$

The matrix from Equation (16) becomes:

$$\begin{pmatrix} 0 & 0 & 1 & 0 \\ 0 & 0 & 0 & 1 \\ \frac{3}{4}\Omega^2 & \frac{3\sqrt{3}}{4}\kappa_\pm\Omega^2 & 0 & 2\Omega \\ \frac{3\sqrt{3}}{4}\kappa_\pm\Omega^2 & \frac{9}{4}\Omega^2 & -2\Omega & 0 \end{pmatrix}$$

with four eigenvalues:

$$\lambda_\pm = \pm i\frac{\Omega}{2}\sqrt{2-\sqrt{27\kappa_\pm^2-23}},$$
$$\sigma_\pm = \pm i\frac{\Omega}{2}\sqrt{2+\sqrt{27\kappa_\pm^2-23}}.$$

By Corollary 1.1.1 and Corollary 1.1.2, it is determined that each of the eigenvalues must be imaginary (otherwise there will necessarily be at least one eigenvalue with $\text{Re}(\lambda) > 0$, making the point unstable), so $\sqrt{2-\sqrt{27\kappa_\pm^2-23}}$ must be completely real. Due to $|\kappa_\pm| \leq 1$, $\sqrt{27\kappa_\pm^2-23} \leq 2$, the only remaining condition is:

$$27\kappa_\pm^2 - 23 \geq 0 \qquad (22)$$

After algebraic manipulation, we end up with:

$$\frac{m_1}{m_2} \geq \frac{1+\sqrt{\frac{23}{27}}}{1-\sqrt{\frac{23}{27}}} = \frac{25+3\sqrt{69}}{2} \qquad (23)$$

This provides the expected condition for the stability of the Lagrange points, L_4 and L_5. □

"Hamiltonian mechanics" replaces the velocities used in Lagrangian mechanics with momenta. Sir William Rowan Hamilton (1834) developed powerful geometric techniques for studying the properties of dynamical systems that permit a much wider class of coordinates than the Newtonian or Lagrangian approaches. Hamiltonians describe the system in terms of components of momentum and coordinates of space and time while still considering the conservation of energy of the system as a whole. Lagrangian mechanics involves one second order ODE while the Hamiltonian approach utilizes two first order ODEs. In addition, Lagrangian mechanics focuses on the configuration space, the representation of all the possible spatial positions of a given system. Hamiltonian mechanics are represented by the phase space, the portrayal of all the possible motion states of a system (Hirvonen, n.d.).

One can derive the Hamiltonian formalism out of the Lagrangian formalism (or vice versa) with a Legendre transformation (Zia et al., 2009):

$$L(v,q) = \frac{1}{2}\langle v, Mv \rangle - V(q), \qquad (24)$$

where (v,q) are coordinates on $\mathbb{R}^n \times \mathbb{R}^n$, M is a positive real matrix, and

$$\langle x, y \rangle = \sum_j x_j y_j.$$

For every q fixed, $L(v,q)$ is a convex function of v, while $V(q)$ acts as a constant. Hence, the Legendre transform of $L(v,q)$ as a function of v is the Hamiltonian function,

$$H(p,q) = \frac{1}{2}\langle p, M^{-1}p \rangle + V(q). \qquad (25)$$

For the Two-Body Problem, the real-valued function $H(q,p)$ takes its domain on the $2n$-dimensional phase space. The solution of this Hamiltonian yields results that are consistently obtainable in these integrable single degree of freedom systems (Holmes, 1990). This approach breaks down when another spatial object is introduced in the Three-Body Problem, which can be formulated as a Hamiltonian system with nine degrees of freedom that can be, at best, reduced to four degrees of freedom by using all 10 classical integrals of motion. However, the general problem is still intractable (Arrowsmith & Place, 1992).

The nine degrees of freedom are determined by nine coupled second order nonlinear ordinary differential equations (ODEs) (Krishnaswami & Senapati, 2019):

$$m_a \frac{d^2 r_a}{dt^2} = \sum_{b \neq a} Gm_a m_b \frac{r_b - r_a}{|r_b - r_a|^3} \qquad (26)$$

with position vectors r_a for $a = 1, 2, 3$. The seven independent conserved quantities are provided by the three components of momentum, three components of angular momentum, and energy. Due to the generally unpredictable motions of the three bodies, closed-form solutions to the problem are unlikely to be found (Musielak & Quarles, 2014). To remedy this problem, numerical methods are employed, an example of which is the use of series expansions. These expansions yield approximate solutions that converge slowly, limiting their usefulness.

Another approach to solving the Three-Body Problem analytically is by treating it as a restricted Three-Body Problem. One can simplify the problem by assuming that there are two large bodies that travel in circular orbits on a plane with a third body that is much smaller. When evaluating the small body relative to a rotating coordinate system with x-axis as the relative position vector of the two larger bodies, the smaller body is understood to have two degrees of freedom and its equations of motion consist of a single integral.

Well-versed in celestial mechanics, Henri Poincaré became the first mathematician to identify a chaotic deterministic system while studying the Three-Body Problem. In the 1880s, Henri Poincaré discovered aperiodic orbits that are neither monotonically increasing nor approaching a fixed point. He was awarded the prize of King Oscar II of Sweden and Norway for his contributions to the Three-Body Problem (Alligood et al., 2010). His work was notable both for his presentation of the Recurrence Theorem and for laying the basis for local and global analysis of nonlinear differential equations. The Poincaré Recurrence Theorem states that specific dynamical systems will return to a state arbitrarily close to their starting point after a finite amount of time, contributing significantly to our understanding of orbits as dynamical systems (Poincaré, 1993). Other analytic techniques in this work include Poincaré maps, stability theory for fixed points, and studies of periodic orbits. In addition to orbital mechanics, his work is foundational for studies of dynamics encompassing stable and unstable manifolds.

Within the last few years, new strides have been made in our understanding of the Three-Body Problem by way of statistical approximations. Ginat & Perets (2021) shared a new approximation technique that advanced the understanding of the Three-Body Problem significantly through the use of statistical modeling of stellar encounters. These models study the results of a single object with respect to a binary stellar system, called a binary-single encounter. By viewing these systems as progressions of close triple approaches, Ginat's team models the bound non-hierarchical Three-Body Problem and uses the solution to represent the entire encounter as a 'random walk'. Given the probabilities of movement,

a random walk is a probabilistic technique for determining the most likely location of a point subject to random motions. The model developed by Ginat's team produces statistically significant numerical results for measurements of semimajor axis distribution, the escaper's mass distribution, and the final periapsis distribution, demonstrating the good fit of the random walk approach for use with the Three-Body Problem. In addition, Kol (2021) found that flux-based statistical testing revealed strong evidence for the formalization of the Three-Body Problem in terms of flux-based Three-Body statistical measures. Studies thus far have shown a particularly strong relationship when studying non-hierarchical states of escape probabilities, characteristic exponents for narrow escapes, absorption as a function of binary energy and binary angular momentum, and lifetime distribution.

With respect to the dynamics of a nearly-integrable Hamiltonian system, the Kolmogorov-Arnold-Moser (KAM) Theorem provides conditions under which a chaotic system is restricted in extent (Moser, 2001). This arises in cases involving persistence of quasi-periodic motions under small perturbations. The original theorem, concerned with the stability of motions in Hamiltonian systems, fundamentally lends itself to use in orbital close encounters that may perturb the expected motion in quasi-periodic orbits. The theorem was applied to the Solar System and other n-body problems, but it was found that the problem degenerates for numbers of bodies exceeding three. KAM theory is the basis for understanding chaos in periodic motion as it pertains to orbital perturbation and dynamical mechanics. Recently, Pinzari (2013) developed a rotation-invariant version of the theorem showing how to eliminate the degeneracy of this theorem.

While there is no common, universal definition of mathematical chaos, Gleick (1987) offers three helpful descriptions:

- Complicated, aperiodic orbits,

- Recurring behavior that *appears* to be random in a relatively simple dynamical system,

- Irregular, unpredictable evolution of a deterministic, nonlinear dynamical system.

The result of these properties is a definition of chaotic systems as non-periodic, greatly disordered, and deterministic, while also appearing unpredictable and random. Today, it is clear that a system is chaotic if it has sensitive dependence on initial conditions, which creates large geometric growth in error for a small relative Δt.

The simplest chaotic dynamical system is the Bernoulli shift that is described by Herring & Palmore (1989):

$$x_{n+1} = D\, x_n \quad \mathrm{mod}\ 1 \tag{27}$$

where D is an integer that is larger than 1. In base D arithmetic, x is written as:

$$x = .a_1 a_2..., \tag{28}$$

where $a(i)$ takes the values $[0, 1, .., D-1]$. Therefore, a shift of the base point to the right by one digit with each application and   mod 1 recovers the fractional part is the mapping in base D. This dynamical system on the interval reveals sensitive dependence on initial conditions (x_0) and is classified by a geometric growth of D with each iteration.

As the Solar System is stable for the relatively small timescale over which it is observed by humanity, it is unlikely that any of the planets will collide with each other or be ejected from the system in the next few billion years. However, the planets' orbits are chaotic when evaluated over larger timescales. The timescale for which the dynamical system is chaotic is called its Lyapunov time, which is in the range of 2-230 million years in the case of the Solar System. The Lyapunov time is the inverse of a system's largest Lyapunov exponent (Bezručko & Smirnov, 2010). Aleksandr Lyapunov's influence on the field of dynamics studies should not be understated. He developed many important approximation methods for

nonlinear dynamical systems and created the modern theory of the stability of a dynamical system. Some of these methods make it possible to define the stability of sets of ordinary differential equations (Smirnov, 1992).

1.2. Status Quaestionis

This extensive history in dynamical astronomy built the foundation for modern research in mathematical physics. Well-known physicists associated with Caltech, Konstantin Batygin and Mike Brown, published their research relating to a potential "Planet Nine" in the Kuiper Belt (2016). This paper has faced significant scrutiny and challenges to its legitimacy due to concerns of (likely inadvertent) selection bias. For example, a recent study conducted by Napier et al. (2021) could challenge Brown and Batygin's findings. On the other hand, with the James Webb Telescope recently arriving at its final destination, there is hope in the scientific community that we will be able to collect images of such a Planet Nine, should it exist.

Trujillo & Sheppard (2014) observed thirteen of the most withdrawn objects in the Kuiper Belt. These objects, with respect to an ambiguous orbital feature, shared a similar orbital pattern obtained through the implementation of the Kozai Mechanism. The Lidov-Kozai Effect is the most notable dynamical mechanism for constricting the argument of the periapsis (ω) of a minor plane. The mechanism causes the argument of pericenter of a minor planet to oscillate about either 90° or 270°, which means that its periapse, or closest point to the mass it is orbiting, occurs when the body is farthest from the equatorial plane. Trujillo and Sheppard suggested that a massive outer Solar System perturber may exist that restricts ω for the inner Oort Cloud Objects, which are icy pieces of space debris in the Oort Cloud, a spherical shell of cometary bodies that are believed to surround the sun beyond the orbits of the outermost planets.

Following Trujillo and Sheppard's research,

Madigan & McCourt (2016) presented the idea that the Kuiper Belt could be formed by a cone-like structure that created a self-gravitational instability. As a result of this structure, they proposed that the minor planets experienced inclination instability around one to four Galactic years ago, exponentially growing in inclination, and evolving a narrow distribution in ω centered on 40° for very eccentric orbits up to about 70° for lower eccentricity. This proposed solution was simpler by comparison to the pertuber hypothesis.

In 2016, Batygin & Brown chose six Kuiper Belt Objects (KBOs) from a set of thirteen that were observed to be clustered together, a phenomenon claimed to have resulted from Planet Nine's gravitational pull. KBOs are a subset of Trans-Neptunian Objects (TNOs), a group that also contains scattered disc objects (SDOs) that are more heavily influenced by the orbit of Neptune than the KBOs studied by Batygin and Brown. This paper became the first in a number that quickly followed on this topic.

Dissent ensued in the scientific community following Batygin and Brown's research on the grounds of supposed selection bias. The Outer Solar System Origins Survey (OSSOS), part of a project underway to determine observational biases that manifest within the detected sample, was conducted from 2013 to 2017 and discovered more than 800 new TNOs (Shankman et al., 2017). Comparing with existing datasets, researchers involved in the project during this period found inconsistencies with the Minor Planet Center data used by Batygin and Brown.

Brown & Batygin (2019) expounded upon their existing research and refined some of their methods; some main points were observational bias in regards to the longitude of the perihelion, orbital pole, and a comparison to the OSSOS Survey. They also refined their simulation and approach. To determine observational bias as a cause of the clusterings, they developed a method of quantifying the observational biases in the observations of longitude of perihelion and the orbital

Table 1. Comparison of TNOs used in BB21, Napier, and MD

Batygin & Brown	Napier et al.	Moll & D'Alessio	Object Prelim. Desig.	Semi-Major Axis a, (AU)	Perhihelion Distance q, (AU)
(1)	(2)	(3)	(4)	(5)	(6)
✗	✓	✗	$2015BP_{519}$	448.8	35.2
✗	✓	✗	$2013SL_{102}$	314.3	38.1
✓	✓	✓	$2013RA_{109}$	462.4	46.0
✗	✓	✓	$2014WB_{556}$	289.1	42.5
✗	✓	✗	$2016SG_{58}$	233.0	35.1
✓	✓	✓	$2013SY_{99}$	733.1	50.1
✓	✓	✓	$2015RX_{245}$	426.4	45.7
✗	✓	✗	$2015GT_{50}$	311.4	38.5
✗	✓	✗	$2015KG_{163}$	679.7	40.5
✗	✓	✗	uo5m93	283.0	39.5
✓	✓	✓	$2013FT_{28}$	295.4	43.4
✓	✓	✓	$2014SR_{349}$	296.6	47.7
✗	✓	✗	$2015TG_{387}$	1101	65.1
✗	✓	✗	$2014FE_{72}$	1560	36.2
✓	✓	✓	$2012VP_{113}$	262.7	80.5
✗	✓	✗	$2013RF_{98}$	363.6	36.1
✓	✗	✓	$2000CR_{105}$	218.0	43.9
✓	✗	✓	$2003VB_{12}$	479.0	76.4
✓	✗	✓	$2004VN_{112}$	319.0	47.3
✓	✗	✓	$2010GB_{174}$	351.0	48.6
✓	✗	✓	$2013UT_{15}$	197.0	44.1
✗	✗	✓	$2016SD_{106}$	384.1	42.7
✗	✗	✓	$2018VM_{35}$	256.6	45.1

NOTE—It can be seen that a number of the objects noted by Napier et al. (2021) have a perihelion distance of less than 42 AU. Brown & Batygin (2021) share a concern that if objects with $q < 42$ AU are included, the orbits are affected more by Neptune than Planet Nine, making the analyses of these orbits harder to gauge.

pole position. The paper offered a rebuttal to the OSSOS analysis by stating that the OSSOS researchers also impose biases by assuming a specific distribution for the orbital elements of distant objects.

We note that this research still faces skepticism related to selection bias. Napier et al. (2021) resurfaced these issues once again following Batygin & Brown's "new" analysis. Napier et al. explained that Batygin and Brown observed only a small portion of the sky at a specific time, during a specific year. This observation by Napier resurfaces the prior concerns of selection bias that

Batygin and Brown received following their first paper in 2016. Napier and his team selected 14 TNOs from the Outer Solar System Origins Survey, the Dark Energy Survey, and a third that used various telescopes. These objects are indicated in Table 1.

Brown & Batygin (2021) responded to this criticism, publishing a new set of results, in which the two updated their bias approach and outlined new simulation techniques, building upon prior approaches. With new clustering data through the adjustment of sampling techniques, Batygin and Brown updated their statistical significance

of observed clustering to 99.6%, where 2019 significance computation showed 99.8%. This new clustering analysis arose following a few notable changes to their approach. First, Batygin and Brown outline the implementation of a Gaussian Process emulator in a Markov Chain Monte Carlo analysis. This process is applied to a new set of KBOs that is obtained by limiting objects to those with a semi-major axis $150 < a < 1000$ AU and perihelion $q > 42$ AU, leaving a smaller sample of 11 objects. With this new approach, Batygin and Brown find reason to uphold and update their analysis from previous work and outline the parameters of Planet Nine as they reflect simulation data.

2. Methods

To investigate the claims of selection bias made by Napier et al. about the KBOs used by Batygin and Brown, we utilize the JPL Small-Body Database (SBDB) to run a query from the parameters given in Brown & Batygin (2021). This query returns a list of 14 KBOs with both semi-major axis $150 < a < 1000$ AU and perihelion distance $q > 42$ AU. Table 1 displays the 14 objects used in Napier et al. (2021), 11 in Brown & Batygin (2021), and the 14 in our paper.

2.1. Universe Sandbox for Orbit Propagation

In Universe Sandbox, we input the orbital parameters for 14 different KBOs obtained from the SBDB and Horizons propagation software in tandem. The individual masses are not known for most of these KBOs, so the known mass of another small object was used as a placeholder before a statistical approximation could be made.

Figure 1 displays two different perspectives of Planet Nine with these various KBOs, the Sun, and other planets at the end of a 500-year propagation period. Universe Sandbox is programmed as a realistic, physics-based space simulator with unrivalled graphics. Unsurprisingly, with the required computing power for maintaining graphi-

cal performance, Universe Sandbox makes use of Euler's method for n-body orbit propagation, only storing 3-4 significant figures and limiting its usefulness as a tool for studying high-precision perturbations. However, it is useful to visualize the position and orbit of Planet Nine in the context of the other objects being observed directly. Use of the Runge-Kutta Method at the fourth order could prove to make this technique more reliable, leaving an option for further study.

2.2. Mathematica for Orbit Propagation

Using Mathematica, we were able to implement an 11-body simulation with the Sun, Planet Nine, and various KBOs, along with a 10-body simulation containing the Sun and KBOs. Figure 2 shows the final frame of the 11-body simulation.

These simulations are run for the duration of the orbital period of Neptune arbitrarily with the position vector, velocity vector, and mass of each body. For the mass of Planet Nine in the simulation, we obtained the value of 2.98600×10^{25} kilograms, or five times the mass of Earth, from Batygin and Brown's most recent paper. In order to find the hypothesized planet's position and velocity vectors, we utilized Matlab. To do this, we needed Keplerian orbital elements for the objects. Keplerian orbital elements, or Classical Orbital Elements (COEs), comprise a set of information that is commonly used to describe the orbit of a given object in space relative to the Sun. The following list comprises a common group of COEs that were used to compute the information we needed in Matlab:

- a : Semi-major Axis, the size of the orbit

- e : Eccentricity, the shape of the orbit

- i: Inclination Angle, the angle of the orbit plane to the central body's equator

- ω : Argument of Perigee, the angle from the ascending nodes to perigee point
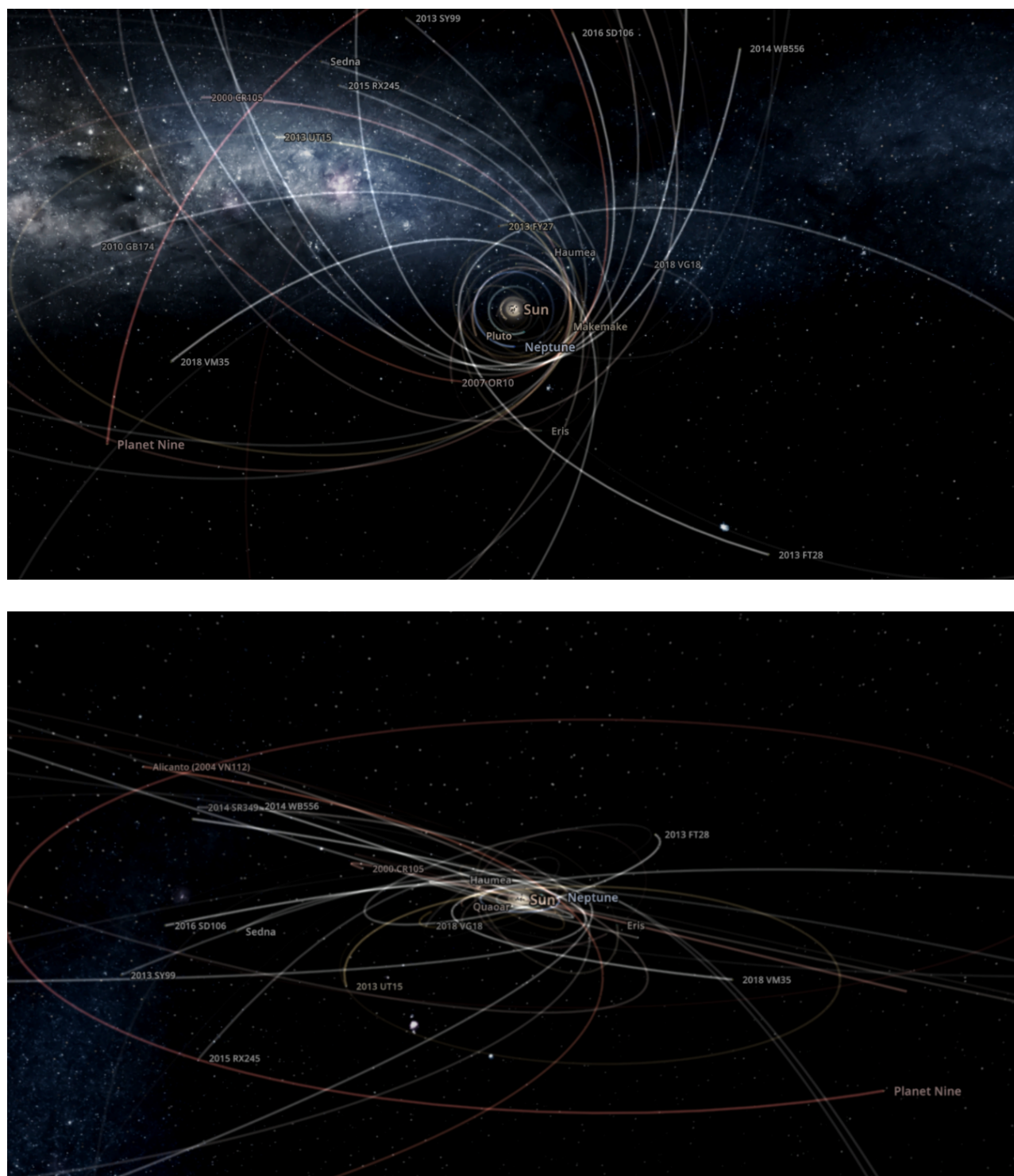
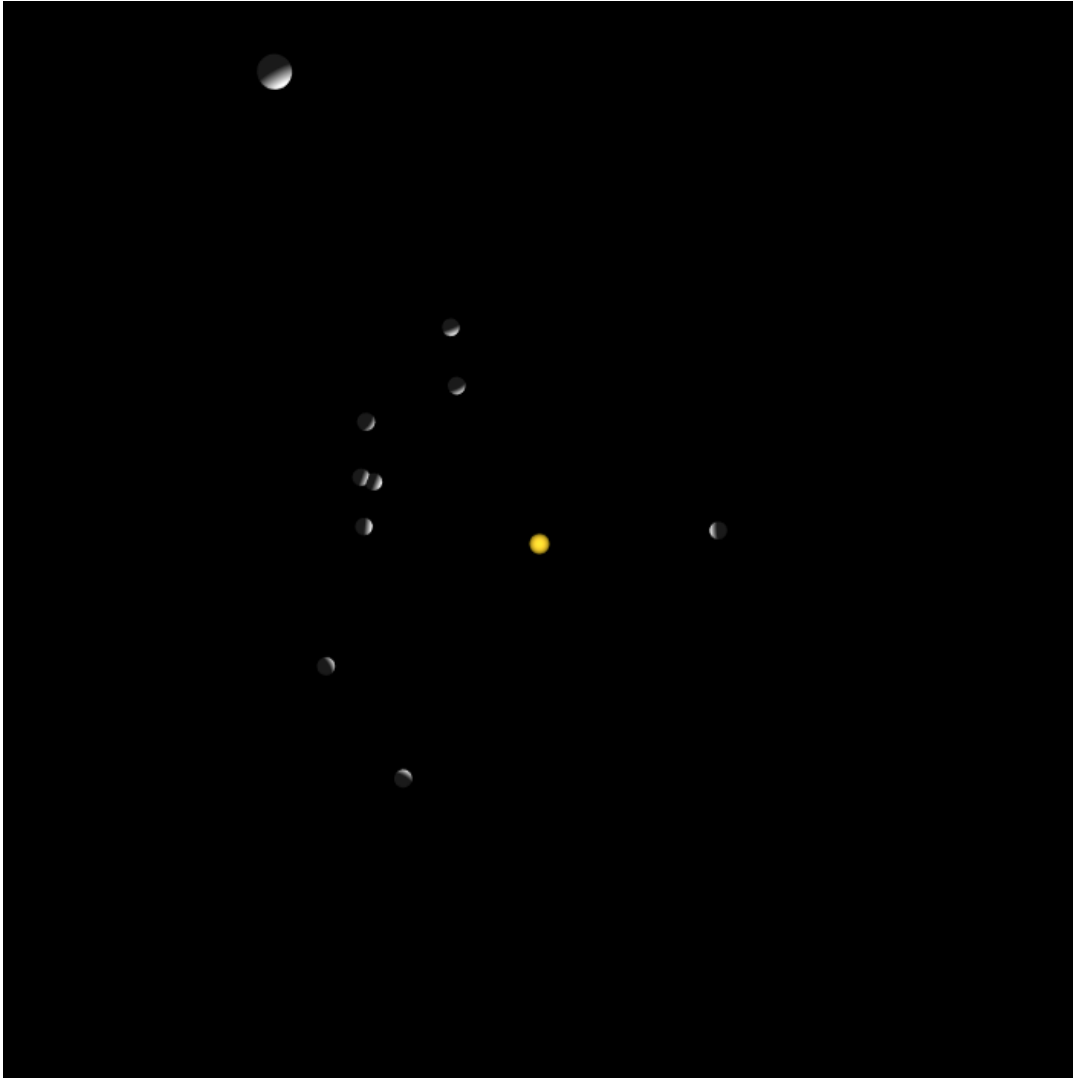Fig. 1. Captures from the Universe Sandbox Simulation

Fig. 2. This is the output of final position of the 11-body simulation with the Sun, Planet Nine, and various KBOs. Note that the duration used in this simulation is the duration of Neptune's solar orbit, 164.79132 Julian Years.

- ν : True Anomaly, the position of the planet on its orbit

- Ω : Right Ascension of the Ascending Node, the rotation of the orbit plane from reference axis.

With this information, we computed instantaneous position and velocity vectors for Planet Nine, the KBOs, and the Sun. These vectors, along with KBO and Sun parameters, comprised the information needed to create the simulations in Mathematica. Excluding Planet Nine from the simulation, the final image produced looks to be the same *sans* the ninth planet, but closer evaluation of final positions revealed perturbations of position in the fifth decimal place. Mathematica's ability to store such precise data is its biggest strength. Ultimately, the Mathematica simulations fail to account for the high eccentricities in the orbits of these KBOs, instead treating the orbits as
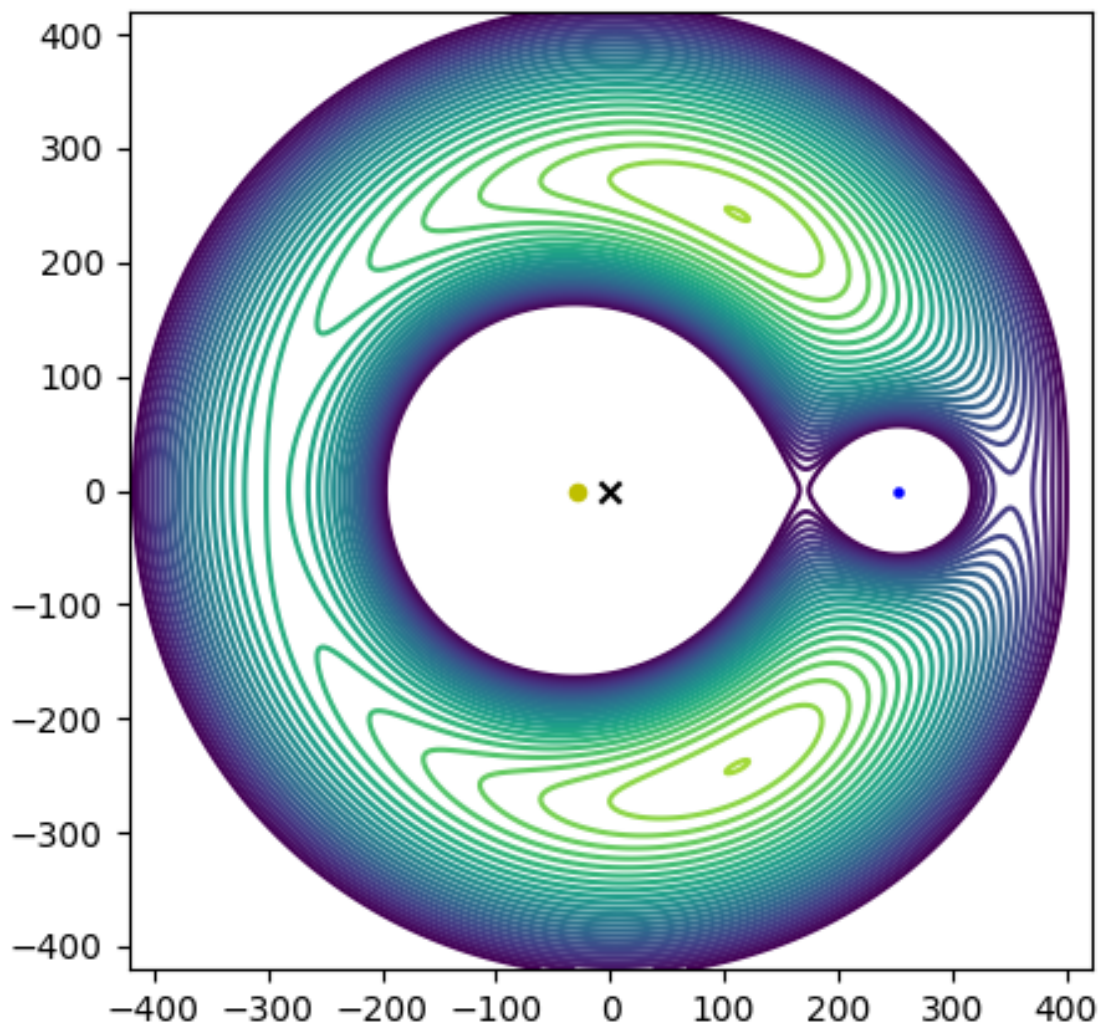
Fig. 3. The Contour plot of the Sun, Planet Nine, and the five Lagrange points

circular, merely computing the effects of Planet Nine's presence on the objects as they pass it on a plane. Regardless, the influence of Planet Nine was unmistakably disclosed in the position vectors.

2.3. Python Lagrange Contour Plot

A contour plot was programmed in Python by making use of matplotlib and NumPy packages. The code outputs Figure 3.

The value of R is given by the distance be-

tween the Sun and Planet Nine, which is assumed to be approximately 280 AU in this case. The equal spacing in the value of $\mu = 0.1$ is represented by the contour lines. The areas where the contour pushes away from or toward an open space are the locations of the Lagrange points. From this contour plot, we can determine the dynamics of the system. Lagrange points 1, 2, and 3 are at saddle points and are in line with the planet and the Sun. Lagrange points 4 and 5 reside at local maxima.

```python
1  import numpy as np
2  import matplotlib.pyplot as plt
3
4  mu = 0.1
5  R = 280
6  sun_pos = np.array([-mu*R, 0])
7  planetnine_pos = np.array([(1-mu)*R, 0])
8
9  N = 1500
10 x, y = np.meshgrid(np.linspace(-1.5, 1.5, N), np.linspace(-1.5, 1.5, N))
11 print(x)
12 print(y)
13
14 term1 = -(1-mu) / ((x + mu)**2 + y**2)**0.5
15 term2 = -mu / ((x - (1-mu))**2 + y**2)**0.5
16 term3 = -0.5 * (x**2 + y**2)
17
18 u = term1 + term2 + term3
19 print(u)
20
21 plt.figure(figsize=(5, 5))
22 levels = np.linspace(-504, -392, 30)
23 plt.contour(x*280, y*280, u*280, levels=levels)
24 plt.scatter([sun_pos[0]], [sun_pos[1]], c='y', s=20)
25 plt.scatter([planetnine_pos[0]], [planetnine_pos[1]], c='b', s=5)
26 plt.scatter([0], [0], c='k', marker='x')
27 plt.axis('equal')
28
29
30
31 plt.savefig('p9_lagrange_contour.png')
```

Fig. 4. Python code for Figure 3.

3. Discussion

Analyzing the differences in the final positions of the KBOs from Mathematica, the results indicate a slight perturbation of orbits for selected objects. We investigated the discrepancies the KBO data used in Batygin and Brown's research with Napier's research to find that there are 14 KBOs in total that satisfy the parameters given by Batygin and Brown in their most recent paper, despite their use of only 11. This emphasizes our goal to address the biases suggested by Napier and others.

In Table 1, it is seen that each KBO referenced by Batygin and Brown is likewise populated in our SBDB query. The objects seen in the SBDB defined by Batygin and Brown's parameters that were not referenced in their paper are 2014WB$_{556}$, 2016SD$_{106}$, and 2018VM$_{35}$. This inconsistency could be caused by a difference in orbital propagation techniques as SBDB uses Horizons. A difference was also clear between the orbital parameters noted by Batygin and Brown and those produced in the Small-Body Data Base.

There are differences in where we obtain our data in comparison to Batygin and Brown and Napier et al. Napier obtains the KBOs from the Outer Solar System Origins Survey, the Dark Energy Survey, and a third that used various telescopes, while Batygin and Brown obtain theirs from the Minor Planet Center (MPC). We used

the JPL Small-Body Database (SBDB) to obtain the data for our simulations. The contour plot created in Python creates a good view of the stability regions in a three-body system including the Sun and Planet Nine with a smaller KBO.

4. Conclusion and Future Considerations

We do not have conclusive results on Planet Nine's existence, but we have a better idea of how the Planet Nine theory fits in our solar system through simulations and the application of dynamical systems theory. Moving forward, we hope to make use of additional computational tools, such as the `mercury6` orbital propagation code or developing new software capable of storing more precise data in a friendly UI. We are also working on a way to approximate KBO masses to make the simulations more accurate. Other future work includes a statistical approximation for the masses of these objects. The total mass of the 31 largest objects in the Kuiper Belt is calculated to be 0.0197 times the mass of Earth, or 5.97219×10^{22} kilograms (Pitjeva & Pitjev, 2018). This information will be used to find a normalized mass that can be attributed to these objects for better evaluation. The quest for Planet Nine continues!

5. Acknowledgements

References

Alligood, K. T., Sauer, T. D., & Yorke, J. A. 2010, Chaos: an introduction to dynamical systems, repr. edn., Textbooks in mathematical sciences (New York, NY Heidelberg: Springer)

Arnol'd, V. I. 1963, Russian Mathematical Surveys, 18, 9

—. 1964, Instability of dynamical systems with several degrees of freedom

Arnol'd, V. I. 1963, Russian Mathematical Surveys, 18, 85–191, doi: `10.1070/RM1963v018n06ABEH001143`

Arrowsmith, D. K., & Place, C. M. 1992, Dynamical systems: differential equations, maps, and chaotic behaviour, 1st edn. (Chapman Hall), 259

Batygin, K., Adams, F. C., Brown, M. E., & Becker, J. C. 2019, Physics Reports, 805, 1, doi: `10.1016/j.physrep.2019.01.009`

Batygin, K., & Brown, M. E. 2016, The Astronomical Journal, 151, 22, doi: `10.3847/0004-6256/151/2/22`

Batygin, K., & Laughlin, G. 2008, The Astrophysical Journal, 683, 1207–1216, doi: `10.1086/589232`

Bezručko, B. P., & Smirnov, D. A. 2010, Extracting knowledge from time series: an introduction to nonlinear empirical modeling, Springer series in synergetics (Berlin Heidelberg: Springer)

Borderies, N., Goldreich, P., & Tremaine, S. 1983, Icarus, 55, 124, doi: `https://doi.org/10.1016/0019-1035(83)90055-6`

Brown, M. E., & Batygin, K. 2019, The Astronomical Journal, 157, 62, doi: `10.3847/1538-3881/aaf051`

—. 2021, The Astronomical Journal, 162, 219, doi: `10.3847/1538-3881/ac2056`

Celletti, A., & Chierchia, L. 2007, Memoirs of the American Mathematical Society, 187, doi: `10.1090/memo/0878`

Chierchia, L., & Mather, J. N. 2010, Scholarpedia, 5, 2123, doi: `10.4249/scholarpedia.2123`

Cornish, N. 1998, The Lagrange Points, NASA GSFC. `https://map.gsfc.nasa.gov/ContentMedia/lagrange.pdf`

Fitzpatrick, R. 2011, Newtonian Dynamics, fourth edition edn. (Lulu)

Ginat, Y. B., & Perets, H. B. 2021, Physical Review X, 11, 031020, doi: `10.1103/PhysRevX.11.031020`

Gleick, J. 1987, Chaos: making a new science (New York, N.Y., U.S.A: Viking)

Greenspan, T. 2014, Stability of the Lagrange Points, L_4 and L_5

Hamilton, W. R. 1834, Philosophical Transactions of the Royal Society of London, 124, 247–308, doi: `10.1098/rstl.1834.0017`

Herring, C., & Palmore, J. I. 1989, ACM SIGPLAN Notices, 24, 76–79, doi: `10.1145/71605.71608`

Hirvonen, V. n.d., Lagrangian vs Hamiltonian Mechanics: The Key Differences. `https://profoundphysics.com/lagrangian-vs-hamiltonian-mechanics/`

Holmes, P. 1990, Physics Reports, 193, 137–163, doi: `10.1016/0370-1573(90)90012-Q`

Jefferys, W. H., & Moser, J. 1966, The Astronomical Journal, 71, 568, doi: `10.1086/109964`

Kepler, J., & Donahue, W. H. 2015, Astronomia nova

Kol, B. 2021, Celestial Mechanics and Dynamical Astronomy, 133, 17, doi: `10.1007/s10569-021-10015-x`

Kolmogorov, A. N. 1954, Proceedings of the USSR Academy of Sciences, 98, 527

Krishnaswami, G. S., & Senapati, H. 2019, Resonance, 24, 87–114, doi: `10.1007/s12045-019-0760-1`

Lagrange, J. L. 1811, Mécanique analytique, 1st edn., Vol. 1 (Paris, Ve Courcier). `https://www.loc.gov/item/04007770/`

Laskar, J., & Robutel, P. 1995, Celestial Mechanics Dynamical Astronomy, 62, 193–217, doi: `10.1007/BF00692088`

Madigan, A., & McCourt, M. 2016, Monthly Notices of the Royal Astronomical Society: Letters, 457, L89, doi: `10.1093/mnrasl/slv203`

Martens, P. 1984, Physics Reports, 115, 315, doi: `10.1016/0370-1573(84)90184-4`

Moser, J. 2001, Stable and random motions in dynamical systems: with special emphasis on celestial mechanics, 1st edn., Princeton landmarks in mathematics and physics (Princeton: Princeton University Press)

Moser, J. K. 1962, On invariant curves of area-preserving mappings of an anulus

Musielak, Z. E., & Quarles, B. 2014, Reports on Progress in Physics, 77, 065901, doi: `10.1088/0034-4885/77/6/065901`

Napier, K. J., et al. 2021, arXiv:2102.05601 [astro-ph]. `http://arxiv.org/abs/2102.05601`

Newton, I., Cohen, I. B., & Whitman, A. M. 1999, The Principia: mathematical principles of natural philosophy (University of California Press)

Njuenje, J., & de Silva, D. S. 2018, The Equations of Planetary Motion and Their Numerical Solution, WIU. `http://www.wiu.edu/cas/mathematics_and_philosophy/graduate/equations-planetary-motion.pdf`

Perko, L. 2001, Texts in Applied Mathematics, Vol. 7, Differential Equations and Dynamical Systems (Springer New York), 182, doi: `10.1007/978-1-4613-0003-8`

Pinzari, G. 2013, arXiv:1309.7028 [math]. `http://arxiv.org/abs/1309.7028`

Pitjeva, E. V., & Pitjev, N. P. 2018, Celestial Mechanics and Dynamical Astronomy, 130, 57, doi: `10.1007/s10569-018-9853-5`

Poincaré, H. 1993, New methods of celestial mechanics, History of modern physics and astronomy (Woodbury, NY: American Institute of Physics)

Shankman, C., et al. 2017, The Astronomical Journal, 154, 50, doi: `10.3847/1538-3881/aa7aed`

Siegel, C. L., & Moser, J. 1995, Lectures on celestial mechanics, Classics in mathematics (Berlin: Springer)

Smirnov, V. I. 1992, International Journal of Control, 55, 775–784, doi: `10.1080/00207179208934258`

Trujillo, C. A., & Sheppard, S. S. 2014, Nature, 507, 471, doi: `10.1038/nature13156`

Westra, D. B. 2017

Zia, R. K. P., Redish, E. F., & McKay, S. R. 2009, American Journal of Physics, 77, 614–622, doi: `10.1119/1.3119512`